

CASE SERIES

DIAGNOSTIC DILEMMA OF PULMONARY MASSE

CORRESPONDING AUTHOR

DR. SHARAD RUNGTA (MD RADIOLOGY)

SENIOR RESIDENT DEPARTMENT OF RADIO-DIAGNOSIS,

SSG HOSPITAL AND MEDICAL COLLEGE BARODA,

VADODARA, GUJARAT-390001

PHONE NO: 7406202541

EMAIL: shadrungtadr@gmail.com

CO-AUTHOR

DR. KIRTI TANTIA (MD RADIOLOGY)

ASSISTANT PROFESSOR DEPARTMENT OF RADIO-DIAGNOSIS,

SSG HOSPITAL AND MEDICAL COLLEGE BARODA,

VADODARA, GUJARAT-390001

DR. SHAILY JANI (MD RADIOLOGY)

SENIOR RESIDENT DEPARTMENT OF RADIO-DIAGNOSIS,

SSG HOSPITAL AND MEDICAL COLLEGE BARODA,

VADODARA, GUJARAT-390001

ABSTRACT

The incidence of malignant disease ranges from 10 to 70% with an average of 40% [1] [2] [3] [4]. As the progression of pulmonary malignancy is high, pulmonary lesions need to be diagnosed early. Solitary pulmonary masses are readily misinterpreted radiologically due to their morphological characteristics. However, many benign lesions can radiologically present as malignant mass lesion.

Here we report 4 such cases who were clinically and radiologically pulmonary malignant mass suspect but eventually turned out to be benign lesions on HPE correlation.

INTRODUCTION

Because lung malignancies progress rapidly, pulmonary lesions should be diagnosed early. Granulomas and bronchogenic carcinomas account for the majority of lung nodules. Other common causes of pulmonary nodules include hamartomas, metastases, infarcts, vascular malformations, focal inflammatory masses, and lipid pneumonia in descending order of frequency [4]. If recent advances in diagnostic imaging and interventional procedures are applied appropriately, surgery can be performed selectively for malignant lesions and people with benign lesions can be treated medically. Surgical resection is not required when benign lesions are definitively diagnosed, but malignant lesions such as lung cancer and solitary metastases are treated by resection [4].

CASE 1

62-year-old male with history of smoking since >30 years presented with right upper back pain and cough for 1 month. On physical examination, patient was cachectic. Laboratory analysis shows normal CBC.

On CXR, inhomogeneous radio-opacity was noted in right apical lung zone with contralateral tracheal shift. HRCT Chest showed ill-defined soft tissue density lesion with air filled cavity within involving right apical lung lobe abutting the superior mediastinum structure with loss of fat plane. (Figure 1)

Further, CECT Chest lesion was heterogeneously enhancing with central non-enhancing area extending into prevertebral space causing osteolytic destruction of T2, T3 and T4 vertebral bodies and showing loss of fat plane with trachea, oesophagus and trachea-oesophageal groove. Right brachio-cephalic vein thrombosis and necrotic pre-paratracheal, pre-para-aortic & aorto-pulmonary window lymphadenopathy was noted.

CT guided lung biopsy was further done for tissue sampling. Histopathological assessments show fibro-collagenous tissue with inflammatory cell infiltrates consisting of lymphocytes and few degraded epithelioid types of cells raising possibility of *Organized healed lesion of Tuberculosis*. No evidence of any malignant cells noted.

CASE 2

61-year-old malnutrition male with long history of DM and smoking presented with severe cough and haemoptysis for 2-3 months.

On CXR, reticular opacity was noted in left mid lung zone with elevated left hemidiaphragm. HRCT Chest showed generalized emphysematous changes with abnormal opacity in left upper lung lobe with broad base towards the mediastinum causing reticulation and plate atelectasis in underlying left lung. (Figure 2)

Further, on CECT Chest heterogeneously enhancing lesion with non-enhancing areas within noted in anterior mediastinum extending into middle mediastinum and left hilum with loss of fat plane with aortic arch (>180 degree), descending aorta (> 90 degree <180 degree), main pulmonary artery (>180 degree) and left pulmonary artery (encasing 360 degree) with luminal compression of pulmonary vessels, left main bronchus and left upper bronchus. Necrotic left supraclavicular and left paratracheal lymphadenopathy noted.

CT guided lung biopsy was further done for tissue sampling. Histopathological sections reveal fibro-connective and fibro-osseous tissue showing inflammatory infiltrates mainly neutrophils, areas of necrosis and haemorrhage. *Aseptate fungal hyphae are seen*. No evidence of any malignant cells noted.

CASE 3

65-year-old chronic male smoker presented with breathlessness, dry cough, hoarseness of voice, weight loss and anorexia for last 6 months. Laboratory analysis shows normal CBC.

On CXR, ill-defined pleural and sub-pleural radio-opacity noted in right upper-mid lung zone with surrounding reticulations. HRCT Chest showed ill-defined soft tissue density lesion with speculated margins and surrounding reticulations. Generalized centrilobular emphysema noted. (Figure: 3)

Direct CT guided lung biopsy was ordered for this patient on strong suspicion of malignancy. Histopathological multiple sections show mainly neutrophilic cell collection with necrosis, pigmented macrophage and fibro-collagenized tissue. No evidence of malignancy is seen in received biopsy bits. Biopsy represents *Acute Suppurative Inflammation*.

CASE 4

55-year-old chronic male smoker presented with cough for 2-3 days, blood in sputum, and generalized weakness for 6-7 months. Laboratory analysis shows minimally raised TC.

On CXR, ill-defined radio-opacity noted in right mid-lung zone extending into right hila. HRCT Chest showed ill-defined soft tissue density lesion with surrounding ground glass opacity and reticulations along minor fissure in anterior segment of right upper lung lobe. (Figure: 4)

Further, on CECT Chest lesion shows heterogeneous enhancement with speculated margins and non-enhancing necrotic areas within.

CT guided lung biopsy was further done for tissue sampling. Histopathological section mainly shows inflammatory cells comprising of lymphocytes and plasma cells within alveoli as well as thickened fibrous septa. Focal area of dense collagenization also seen. Some area shows pigmented alveolar macrophages inside alveoli and atypical pneumocytes in alveolar lining. *Possibility of pneumonia is more.* Definite evidence of malignancy is not seen.

DISCUSSION

Lung lesions greater than 3 cm in size are defined as lung masses [5] [4] [6]. Detection and work-up of lung mass are critical because it may be malignant and lung cancer has an overall mortality rate of up to 85% [4]. Early detection of small nodules may potentially reduce lung cancer-specific mortality.

CRITERIAS TO DIFFERENTIATE BENIGN VS MALIGNANT LESION: -

- | | |
|------------------------------------|---------------------------|
| 1. SHAPE | 2. LOCATION |
| 3. MARGINS | 4. CALCIFICATION |
| 5. CONTRAST ENHANCEMENT COMPONENTS | 6. SOLID AND GROUND GLASS |
| 7. AIR-BRONCHOGRAM SIGN | 8. GROWTH |

BRONCHOGENIC CARCINOMA is the commonest cancer in men and in women it comes after breast, colon and skin cancers. It is a disease usually of the elderly and is rarely considered in the differential diagnosis of lung lesions in those less than 40 years, but is found in all age groups including childhood. The single most important etiological factor is cigarette smoking.

THORACIC ACTINOMYCOSIS accounts for 10–15% of actinomycosis cases and is the third most prevalent location after cervico-facial (60%) and abdominopelvic (20%) region [7]. It can be sub-classified further into pulmonary parenchymal, bronchial, and laryngeal actinomycosis [8]. Of these, pulmonary actinomycosis is the most common [9]. The clinical presentation of pulmonary actinomycosis includes: chest pain, productive cough, shortness of breath, and haemoptysis [10]. Examination findings are usually nonspecific. The imaging modality of choice is usually a CT scan of the chest which typically reveals a mass or peripheral consolidation and associated adjacent pleural thickening at an early stage, and may further demonstrate a trans-fissural extension or abscess formation at a later stage. CXR usually reveals the similar findings of a pulmonary mass. Positron emission tomography

scans are sometimes performed with the intention of differentiating malignant lesions from benign lesions including pulmonary actinomycosis.

Conventional CT scan is the main examination method for distinguishing PULMONARY TB from lung cancer. Diagnosis and differentiation depend on the location, size and shape of the mass, as well as its lobes, borders, density, and enhancement characteristics. Traditional qualitative analysis of CT images involves making preliminary diagnosis based on the characteristics of the mass. However, the diagnostic accuracy is closely related to doctors' experience, judgment of signs is also subjective and limited, lacks quantitative indicators, has poor reproducibility, and is closely related to the physician's experience. Therefore, diagnosis mainly depends on biopsy pathology. With the deepening of research, it is possible to differentiate specific cases of atypical mass-like TB and peripheral lung cancer. In this study, CT plain scan texture feature parameters were used in combination with morphological features to evaluate the differences of parameters between patients with TB and lung cancer. Previous studies have shown that shallow lobes, long burrs, satellite lesions, calcification, and mild or circular enhancement are all the characteristic of mass-like TB [11] [12]. The edge of the mass was formed by the fusion of fibrous cords or protruding caseous nodules. And the superficial lobed and long burrs of cords were common to see. Tuberculosis often has bronchial spread and satellite foci around nodules or masses. Calcification is the most common complication of tuberculosis, mainly distributed around caseous necrosis and cavity wall. The pattern of enhancement is related to the lack of vascular structure in central coagulation necrosis, surrounding by epithelioid cells, giant cells unequal to Langerhans, infiltration of peripheral lymphocytes and proliferation of fibroblasts [13].

Multiple studies have shown that radiomics can be applied to quantitatively evaluate the difference in texture characteristics between peripheral lung cancer and inflammatory masses, with differential diagnostic efficacy [13] [14]. For instance, *Dennie et al.* [15] studied the heterogeneity of lung cancer and infective granulomas, and found differences in texture characteristics between the central area and the edge of the mass. *Chen et al.*'s study [16] on lung adenocarcinoma and inflammatory granuloma reported that the AUC of imaging features within nodules was 0.75, compared to that of 0.80 for the combination of nodule and surrounding histological features, indicating that the omics features around nodules carry great value in the prediction of malignant tumours. *Suo et al.* [17] identified sex and age, irregular edges and lobular features of the lesion, and radiomics features as the main factors for distinguishing lung adenocarcinoma from granulomatous TB, which indicates that the combination of a clinical risk factor model and an imaging features model is of great value for differentiating the two diseases. *Beig et al.* [18] showed that a nomogram based on imaging features from within a 4-mm peripheral radius of the nodule had the highest efficiency for distinguishing lung cancer and TB; in the training group, the AUC was 0.914 (with a sensitivity and specificity of 0.890 and 0.796, respectively), and in the verification group, the AUC was 0.900 (with a sensitivity and specificity of 0.788 and 0.907, respectively). Their observations showed that the 4-mm area around the tumour had a more potent distinguishing value than the intratumoral features.

CONCLUSION

To conclude this chronic pulmonary lesion are known for their notorious behavior because of overlapping imaging features between organized infections and malignant masses. Mimics of ancillary imaging feature such as lymphangitis carcinomatosa, necrotic mediastinal lymphadenopathy and mediastinal/pleural invasion can also be seen in infections like TB and fungal pneumonias. So chronic pulmonary lesions have become a diagnostic deathly hallow for clinicians as well as radiologists. So subtle clinical and radiological signs with Histopathological correlation becomes very important for prompt patient management.

REFERENCES

- [1] D. A. G. R. A. D. Adam A, "Diagnostic Radiology-A textbook of medical imaging. 5th edition," in *Diagnostic Radiology-A textbook of medical imaging. 5th edition*, Churchill Livingstone , Elsevier, 2008, pp. 187-350, 1461-1485.
- [2] S. D., "Textbook of radiology and imaging.7th edition," in *Textbook of radiology and imaging.7th edition*, Churchill Livingstone, Elsevier, 2003, pp. 1-128, 247-262.
- [3] V. S. M. F. R. C. H. K. M. S. Haaga JR, "CT and MRI of the whole body. 5th edition," in *CT and MRI of the whole body. 5th edition*, Philadelphia, Elsevier, 2009, pp. 927-958, 2462- 2486.
- [4] B. K. H. L. J. e. a. Fauci, "Harrison's Principles Of Internal Medicine. 17th edition," in *Harrison's Principles Of Internal Medicine. 17th edition*, New York, McGraw-Hill, 2008, pp. 552-560.
- [5] F. K. K. E. I. M. Tan BB, "The solitary pulmonary nodule. Chest," in *The solitary pulmonary nodule. Chest* , 2003, pp. 123:89s-96.
- [6] M. W. Helen T, "The solitary pulmonary nodule.," *Radiology* , pp. 46, 239:34, 2006.
- [7] K. R. M. L. M. R. M. I. Boyanova L, "Actinomycosis: A frequently forgotten disease," *Future Microbiology*, p. 10(4):613–28, 2015.
- [8] L. K. L. J. e. a. Han JY, "An overview of thoracic actinomycosis: CT features," *Insights Imaging*, p. 4(2):245–52, 2013.
- [9] S. S. K. J. e. a. Heo SH, "Imaging of actinomycosis in various organs: A comprehensive review.," *Radiographics*, p. 34(1):19–33., 2014;.
- [10] H. J. K. W. e. a. 10. Kim TS, "Thoracic actinomycosis: CT features with histopathologic correlation," *AJR American Journal of Radiology*, p. 186(1):225–31, 2006.
- [11] M. D. X. Z. e. a. Li BG, "The value of multislice spiral CT features of cavitory walls in differentiating between peripheral lung cancer cavities and single pulmonary tuberculous thick-walled cavities," *Br J Radiol* , pp. 85:147-52, 2012.
- [12] S. W. Wang XL, "Application of dynamic CT to identify lung cancer, pulmonary tuberculosis, and pulmonary inflammatory pseudotumor," *Eur Rev Med Pharmacol Sci*, pp. 21:4804-9, 2017.
- [13] L. Z. S. G. e. a. Zeng J, "MRI evaluation of pulmonary lesions and lung tissue changes induced by tuberculosis," *Int J Infect Dis*, pp. 82:138-46, 2019.

- [14] H. J. W. J. e. a. Yang X, "CT-based radiomics signature for differentiating solitary granulomatous nodules from solid lung adenocarcinoma.," 2018;125:109-14.
- [15] T. R. S.-V. V. e. a. Dennie C, "Role of quantitative computed tomography texture analysis in the differentiation of primary lung cancer and granulomatous nodules," *Quant Imaging Med Surg*, pp. 6:6-15, 2016.
- [16] F. B. C. Y. e. a. Chen X, "A CT-based radiomics nomogram for prediction of lung adenocarcinomas and granulomatous lesions in patient with solitary sub-centimeter solid nodules," *Cancer Imaging*, p. 20:45, 2020.
- [17] C. J. C. M. e. a. Suo S, "Assessment of Heterogeneity Difference Between Edge and Core by Using Texture Analysis: Differentiation of Malignant From Inflammatory Pulmonary Nodules and Masses," *Acad Radiol*, pp. 23:1115-22, 2016.
- [18] K. M. A. M. e. a. Beig N, "Perinodular and Intranodular Radiomic Features on Lung CT Images Distinguish Adenocarcinomas from Granulomas.," *Radiology* , pp. 290:783-92, 2019.

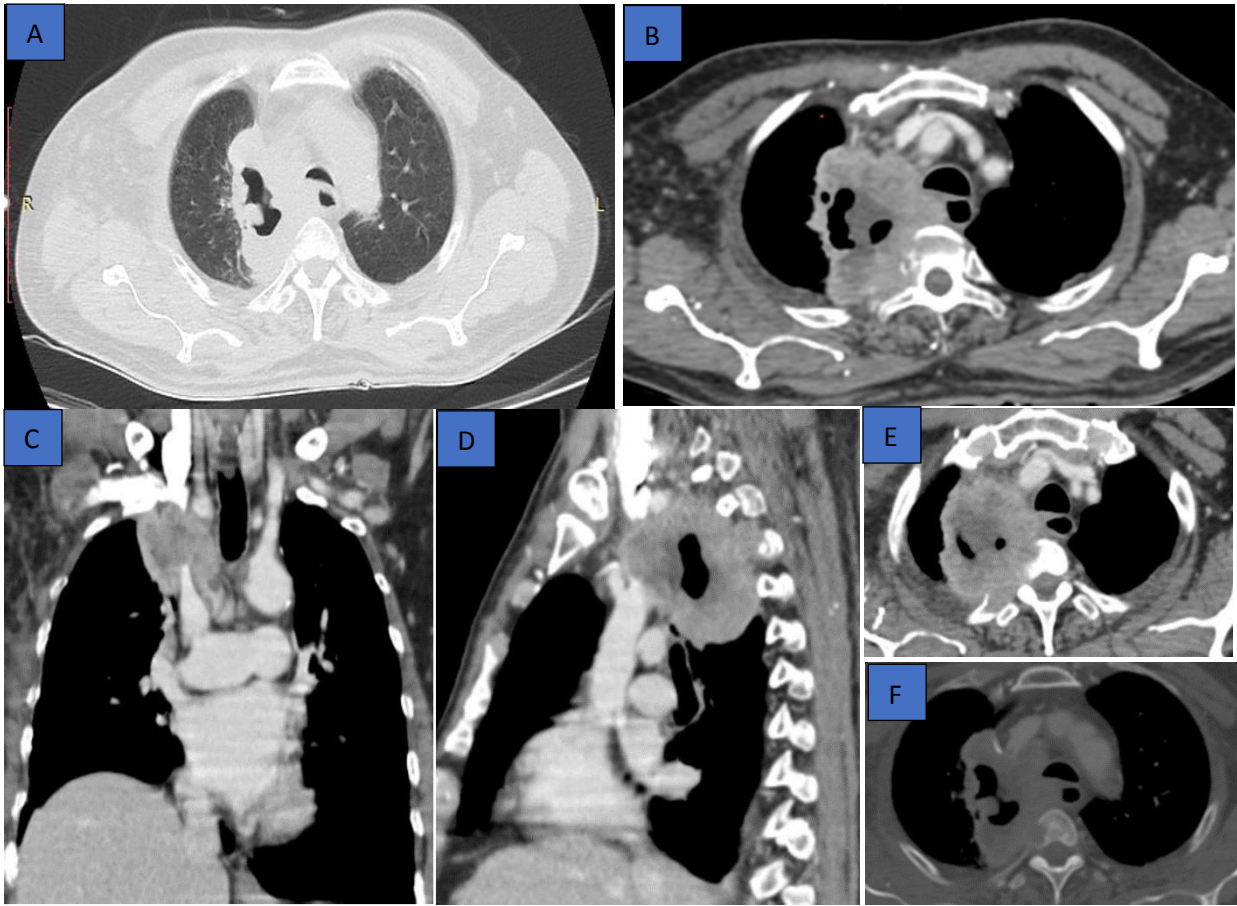


Figure 1. (Case 1) Large lobulated heterogeneously enhancing mass lesion with cavitation and necrotic areas within in right apical lung lobe (A). Mass is seen to abut trachea and Esophagus with loss of fat plane (B). It is also extending focally into right brachiocephalic vein (C & D). Posteriorly lesion is causing osteolytic destruction of vertebral body (E & F).

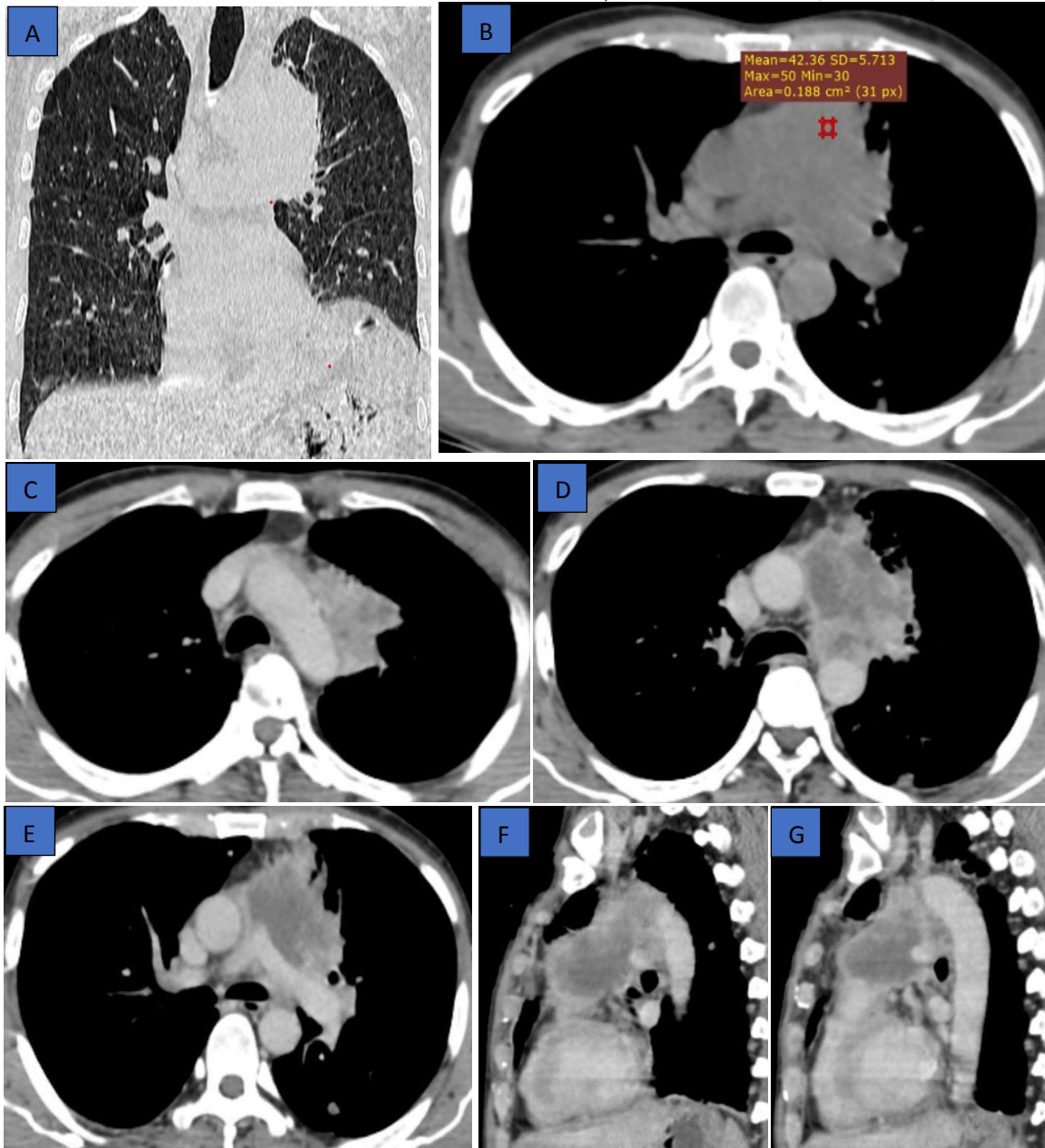


Figure 2. (Case 2) Ill-defined soft tissue density lesion (A & B) with necrotic areas (D-G) in left hilar region extending into middle and anterior mediastinum (D & E). Lesion morphologically resemble like a small cell carcinoma of lung which has typical mediastinal

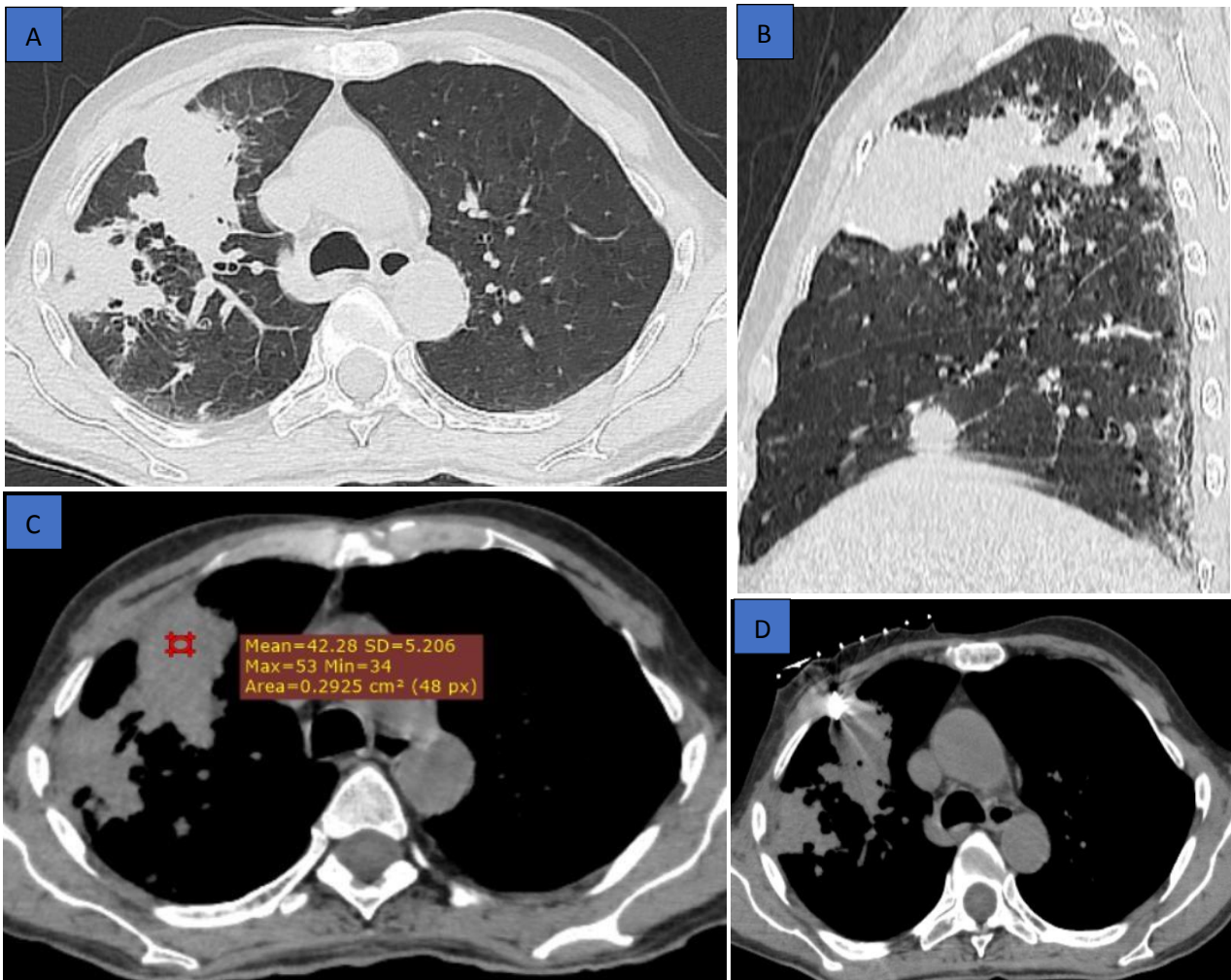


Figure 3. (Case 3) Soft tissue density lesion (C) with spiculated margins (A & B) in right upper lung lobe. Lesion morphologically resemble like an adenocarcinoma of lung. Followed by diagnostic imaging Ct guided biopsy was done (D).

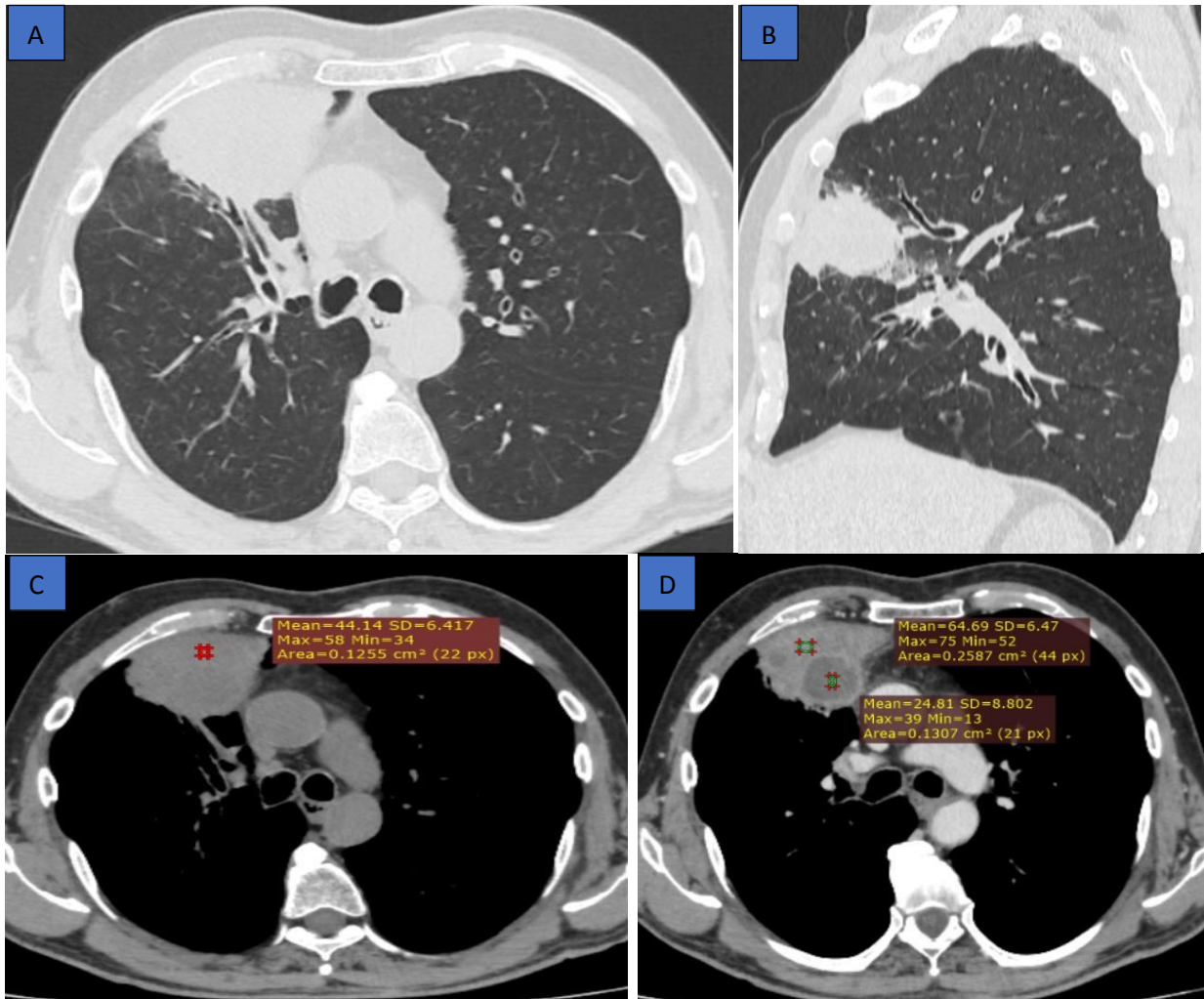


Figure 4. (Case 4) Soft tissue density lesion (A & C) with spiculated margins (B) and cavitation noted in right mid lung lobe with right hilar extension showing heterogenous enhancement and necrotic areas (D). Mass resembles Squamous cell carcinoma morphologically.